Layered Assemblies of Single Crystal Gold Nanoplates: Direct Room Temperature Synthesis and Mechanistic Study

Zhirui Guo,[†,‡] Yu Zhang,[†] Aiqun Xu,[¶] Meng Wang,[†] Lan Huang,[†] Kang Xu,[†] and Ning Gu*[,†]

State Key Laboratory of Bioelectronics and Jiangsu Laboratory for Biomaterials and Devices, Southeast University, Nanjing 210096, China, The Institute of Cardiovascular Disease, the First Affiliated Hospital of Nanjing Medical University, Nanjing 210029, China, and The Analysis and Testing Center, Southeast University, Nanjing 210096, China

Received: April 3, 2008; Revised Manuscript Received: June 26, 2008

Layered assemblies of single crystal gold nanoplates are directly synthesized in large scale by simply adding aniline to $HAuCl_4$−HCl aqueous solution at room temperature, without the need of extra capping agent or surfactant. In this approach, the large amount of Cl^-, the oxidative etching by the O_2/Cl^- pair, the protonation of aniline, and the mild reaction temperature cocontribute to greatly slow up the reduction process of $AuCl_4^-$ for facilitating the formation of these anisotropic gold nanostructures. The as-synthesized layered assemblies consist of inseparable gold nanoplates interconnected via steps between layers, which are confirmed by SEM and TEM. Moreover, these layered assemblies are further characterized by EDX, SAED, FT-IR, XRD, and UV−vis−NIR, respectively. The effects of different synthetic parameters on the shape and size of the final gold product are investigated. On the basis of a series of experimental results, it is revealed that in situ produced polyaniline with rigidly straight chain molecular structure plays a key role in achieving these gold layered assemblies. The possible growth mechanism is also proposed.

Introduction

Since the emergence of nanoscience, metal nanoparticles have gained enormous attention because of their unique electronic, optical, magnetic, thermal, catalytic, as well as other properties not seen from the corresponding bulk solid.[1] Both experimental observations and theoretical calculations have indicated that such properties are highly sensitive to their shapes.[2] One example is that the shape of gold nanoparticles can drastically change the surface plasmon resonance (SPR) properties. Typically, gold nanorods exhibit two SPR bands (namely transverse and longitudinal plasmon resonances, respectively) arising from their anisotropic shape, whereas only one SPR band is observed for spherical gold nanoparticles due to their high symmetrical shape.[3] As for metal nanoparticles catalysis, Wang and Sun have demonstrated that tetrahexahedral platinum nanoparticles enclosed by high-index facets such as {730}, {210}, and/or {520} exhibit quite enhanced catalytic activity than sphere-like platinum nanoparticles enclosed by {111} and {100} facets for electro-oxidation of small organic fuels.[4] Thanks to the efforts of numerous research groups, many differently shaped metal nanoparticles, including zero-dimensional (0D),[1b,d,5] 1D,[6] 2D,[7] and other complex shapes such as nanomutlipods or nanostars[8] have been synthesized up to now. On the other hand, it is also essential to fabricate assemblies at one, two, or three dimensions by using the shape-controlled metal nanoparticles as building blocks, because such structures not only display novel collective behaviors different from those of individual nanoparticles but also are a crucial approach to constructing nanodevices.[9] To the best of our knowledge, 1D, 2D, or 3D assemblies composed of 0D metal nanoparticles have been extensively studied and reviewed,[10] whereas fabricating ordered assemblies of the metal nanoparticles with anisotropic shape has been met with limited success and is mainly concerned with gold nanorods.[11]

In recent years, single-crystal 2D gold nanoplates with a large flat top and bottom enclosed by {111} facets are of great interest due to their promising applications as gas sensors,[12] near-infrared (NIR) light absorbers for cancer hyperthermia,[13] platforms for surface-enhanced Raman scattering,[14] and high-resolution scanning tunneling microscopy,[15] as well as blanks for nanomatching.[16] During the evaporation of gold nanoplates solution, people often observe that some nanoplates assemble face to face into layered structures like the stack of rows, with their basal planes parallel to the supporting substrate.[7d,f,h] Unfortunately, these gold layered assemblies formed randomly and were prone to collapse into dispersed ones again, hindering further investigation into their potential properties. As an attempt, Malikova et al. adapted the layer-by-layer (LBL) assembly technique to fabricate multilayered architecture of gold nanoplates.[17] Briefly, negatively charged gold nanoplates mixed with small gold nanoparticles were synthesized by reduction of $AuCl_4^-$ with salicylic acid in aqueous solution. Then the LBL assembly procedure was performed by sequential dipping of a glass slide in aqueous solutions of positively charged polyelectrolyte and these negatively charged gold nanoplates. However, this LBL approach actually resulted in multilayered thin films of gold nanoplates, but not the above-mentioned gold layered assemblies in a face-to-face manner. For the past several years, this has been a challenge for developing a facile method to fabricate the layered assemblies of gold nanoplates. More recently, Yuan et al. reported a wet-chemical approach for the preparation of layered assemblies of gold nanoplates by mixing $HAuCl_4$ and doped sulfonated polyaniline (SPAIN) nanotubes in aqueous solutions at room temperature.[18] Unlike the usual ones of separable gold

* Corresponding author. Phone: +86-25-83794960. Fax: +86-25-83274960. E-mail: guning@seu.edu.cn.

† State Key Laboratory of Bioelectronics and Jiangsu Laboratory for Biomaterials and Devices, Southeast University.

‡ The Institute of Cardiovascular Disease, the First Affiliated Hospital of Nanjing Medical University.

¶ The Analysis and Testing Center, Southeast University.

10.1021/jp8028962 CCC: $40.75 © 2008 American Chemical Society
Published on Web 07/31/2008

nanoplates, these gold layered assemblies from Yuan's approach are composed of inseparable gold nanoplates connected to each other by steps between layers. For this reason, these gold layered assemblies can remain stable in powder or suspension state, facilitating subsequent investigations. As suggested by Yuan, the doped SPANI nanotubes serve as not only a reductant but also a capping agent to direct the shape of gold nanoparticles.[18] However, there still exist ambiguities about the formation mechanism of these layered assemblies. Furthermore, when employing Yuan's approach, the commercially unavailable SPANI nanotubes have to be presynthesized in the laboratory and the doped SPANI nanotubes always aggregate in the reaction solution because of their water insolubility. Therefore to clarify the formation mechanism and achieve a high production of these interesting structures with low cost, a simple but effective synthetic approach should be more helpful.

Aniline has long been used as a monomer for the synthesis of a technologically important polymer: conductive polyaniline.[19] During the past few years, the synthesis of spherical gold nanoparticles with aniline as both reductant and subsequent stabilizer, in the form of polyaniline, has also been reported.[20] Most recently, our group developed a novel but facile method for a variety of anisotropic gold nanostructures based on the reduction of $HAuCl_4$ by aniline in aqueous solution, without extra capping agent and surfacant.[21] In particular, we also obtained these gold layered assemblies of inseparable single crystal nanoplates in large scale via simply adding hydrochloric acid (HCl) to the reaction solution at room temperature. In the present work, we extend this research to gain an insight into the formation mechanism of these gold layered assemblies and reveal the effects of synthetic parameters on the shape and the size of the gold nanostructures. The as-synthesized gold layered assemblies were characterized by using various spectroscopic and microscopic techniques. It is found that the generation of the gold layered assemblies undergoes a slow-growth process and the in situ produced polyaniline with a rigidly straight chain molecular structure is crucial to achieving these assemblies. A mechanism to explain the growth of gold layered assemblies is proposed, which is also applicable for those obtained by Yuan's approach.

Experimental Section

Materials. Hydrogen tetrachloroauric acid ($HAuCl_4 \cdot 4H_2O$, 99.9%), aniline, hydrochloric acid (HCl), nitric acid (HNO_3), perchloric acid ($HClO_4$), sulfuric acid (H_2SO_4), and anhydrous ethanol were purchased from Shanghai Chemical Reagent Co. Ltd. (China). Poly(vinylpyrrolidone) (PVP, MW 40 000) was supplied by Kitta Co. Ltd. (Japan). Millipore-quality water (18.2 MΩ/cm) was used throughout the experiments. Aniline was distilled and stored in a brown bottle before usage. Other materials were used as received.

Synthesis of Layered Assemblies of Gold Nanoplates. Typically, for the synthesis of layered assemblies of gold nanoplates, 50 mL of aqueous 0.72 mM $HAuCl_4$ at a pH of 1.0 adjusted by 1 M HCl solution was added to a flask, after which aqueous 0.1 M aniline was rapidly added to yield a 3:1 molar ratio of aniline to gold under constant stirring at room temperature. After 24 h the gold product was isolated by centrifuging the resulting solution at 6000 rpm for 20 min and washed three times with ethanol followed by water. Then the product was redispersed in water for further characterization.

The investigation of the effects of different synthetic parameters on the shape and size of the final gold nanostructures was also conducted. Each synthesis followed a similar procedure to that mentioned above for the generation of the layered assemblies of gold nanoplates, except that a certain synthetic parameter, including the amount of aniline, the initial pH value of aqueous $HAuCl_4$, the reaction temperature, and the inorganic acid used for modifying the pH value, was changed, respectively.

Instrumentation. Transmission electron microscopy (TEM) images and selected area electron diffraction (SAED) patterns were taken with a JEM-2000EX (JEOL) transmission electron microscope operated at 120 kV. The samples of the final gold products were prepared by dropping the dispersion onto the carbon-coated copper grid and dried in ambience. To investigate the real shape of the gold intermediates at different reaction stages, the samples were obtained by immersing a carbon-coated copper grid into the solution and immediately transferring it on a filter paper for rapid removal of the excess liquid. Scanning electron microscopy (SEM) images were captured by using a 1530VP (LEO) field-emission scanning electron microscope with an accelerating voltage of 5.0 kV. Energy-dispersive X-ray (EDX) analysis was performed by an INCA energy spectrometer (Oxford) attached to the SEM. A powder X-ray diffraction (XRD) pattern was carried out with a D/Max-RA (Rigaku) instrument, using Cu Kα radiation at room temperature. The sample was deposited onto a silicon wafer and scanned in the 2θ range of 30−90°. The Fourier transform infrared (FTIR) spectrum was measured on a Magna FTIR-750 (Nicolet) spectrometer and the vacuum-dried sample was made in the form of a KBr pellet. The UV−vis−NIR spectra were recorded on a UV-3150 (Shimadzu) spectrophotometer.

Results and Discussion

As shown in Scheme 1, gold atoms can be produced by reducing $AuCl_4^-$ with aniline and then aggregate into seeds followed by further growth. Meanwhile, the oxidized aniline can continually be reduced by free aniline to form dimer, then trimmer, and so on through an oxidative polymerization process including initiation, propagation, and termination.[22] On the condition of strong acid medium and ambient temperature, the oxidative polymerization of aniline results in high molecular weight polyaniline with rigidly straight chain structure.[23]

In the synthesis of gold nanoparticles, when $AuCl_4^-$ is reduced to generate gold atoms very quickly, the shape of the final gold product will take the thermodynamically favored one such as cubooctahedra. However, when the reduction rate becomes slow enough, kinetic control will take over in both nucleation and growth and the final gold product will take shapes deviating from the thermodynamically favored one.[24] Thus to achieve anisotropic gold nanoparticles, one should carefully slow up the reduction process of gold precursor. For this regard, we conduct the synthesis in strong acid solution by adding aqueous HCl at room temperature. First, an ambient temperature condition favors a slow reduction rate. Second, the reduction potential of aniline is pH dependent during its initial oxidative stage, which increases on decreasing the pH of the solution due to its protonation (pK_a of aniline is 4.6),[23] possibly making the reduction of $AuCl_4^-$ proceed in a mild way. On the other hand, the gold seeds are mainly bounded by a mixture of low-index facets for a lowest total surface energy and the sequence of surface energies for low-index facets is $\gamma_{\{111\}} < \gamma_{\{100\}} < \gamma_{\{110\}}$.[25] During the crystal growth, gold atoms tend to add on the facets with higher surface energy to release more energy. In general, the shape of face-centered cubic (fcc) metal nanostructures is mainly determined by the growth rate in the ⟨111⟩ direction to that in the ⟨100⟩ direction.[25] However, for the fcc metals, the low-energy {111} and {100} facets hold similar surface

SCHEME 1: The Reduction of $AuCl_4^-$ by Aniline To Form Gold Nanoparticles and the Oxidative Polymerization Process of Aniline Proceeding through the Loss of Electrons

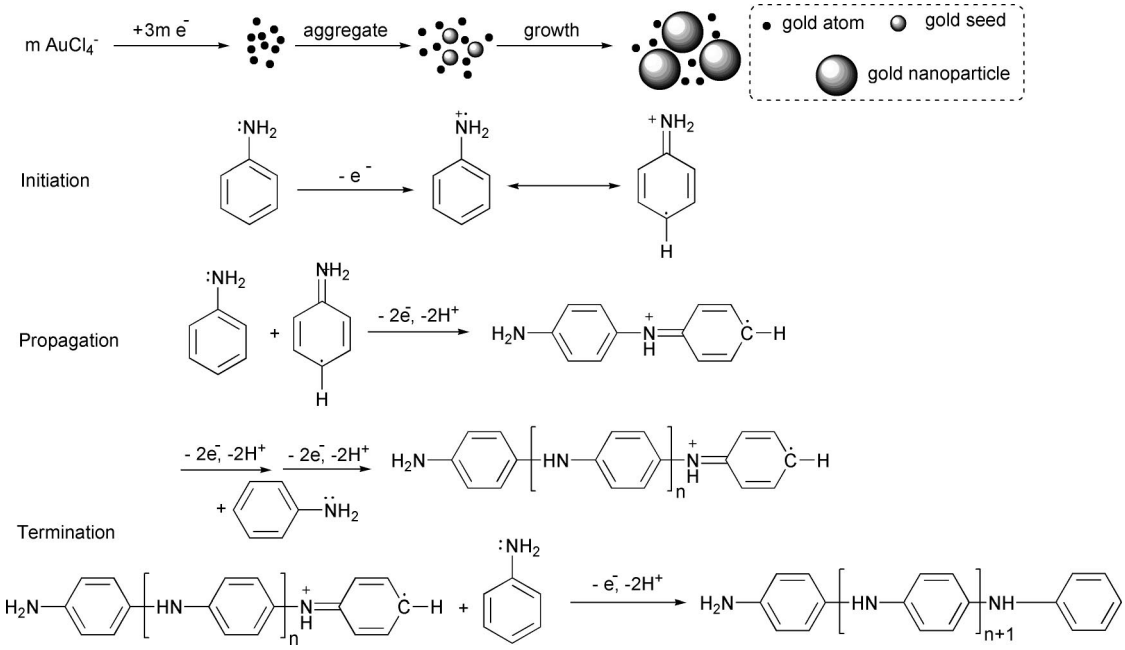

energies; in the case of gold, these energies are 0.886 and 1.083 J m^{2-}, respectively.[26] Therefore without physical confinement, the usual strategy for producing anisotropic gold nanostructures during seed growth is selectively adsorbing specific facets through a capping agent to highly promote the growth of the other facets.[27] As an aromatic amine, aniline is easily dissolved in water and its amino group can interact weakly with metal surfaces. Moreover, a recent study by Tan et al. reveals that a large amount of aniline as stabilizer can direct the growth of the silver nanoparticles to form silver nanoplates.[28] Thus, it is reasonable to predict that the in situ produced polyaniline under slow reaction rate by our case might take a similar function as that of aniline to induce the formation of anisotropic gold nanostructures.

Structural Characterization of Layered Assemblies of Gold Nanoplates. The morphology of the final gold product was first characterized by SEM. The lower magnification image (Figure 1a) reveals the formation of the layered assemblies of truncated triangular- or hexagonal-shaped plates with about 1−3 μm in edge length. The higher magnification image (Figure 1b) shows that these plates are about 20−50 nm in thickness, revealing that they are nanoplates. Furthermore, the image of a single assembly at higher magnification (Figure 1c) clearly shows there are steps on the basal surface of the gold nanoplates, and the upper gold nanoplates epitaxially grow from the steps, orienting parallel to the subjacent nanoplate. Because they interconnect with each other by these steps, these gold nanoplates in the assemblies are inseparable even under ultrasonic treatment on their dilute suspension. The EDX spectrum recorded from the basal planes of these gold nanoplates shows a strong peak due to gold. Moreover, quite weak peaks ascribed to carbon and nitrogen respectively are also observed (Supporting Information, Figure S1), thus indicating that these gold plates are almost pure metallic gold covered with a minute quantity of the result with aniline. The result with aniline was further analyzed by FTIR (Supporting Information, Figure S2). The broad absorption peak located at 3450 cm^{-1} could be assigned to the N−H stretching mode, while the two sharp bands positioned at 1500 and 1598 cm^{-1} are characteristic of the stretching deformation modes of N−B−N (B: benzenoid ring) and N═Q═N (Q: quinoid ring) groups of polyaniline, respectively.[20b,c] These results suggest that these gold nanoplates are covered with the in situ produced polyaniline.

Figure 2a,b gives typical TEM images of individual gold assemblies with different shapes. Due to the low contrast appearance of these thin gold plates, one can clearly observe the multilayered structure of these gold assemblies. Figure 2c shows the SAED pattern by focusing the electron beams perpendicular to the basal plane of a single gold nanoplate in a layered assembly. The hexagonal symmetry of the diffracted spots suggests that the gold nanoplate is a single crystal with atomically flat {111} facets as basal planes.[7] The crystal nature of these gold layered assemblies was also analyzed by XRD (Supporting Information, Figure S3). A strong diffraction peak is found at 38.12° assigned to the {111} lattice facet of fcc

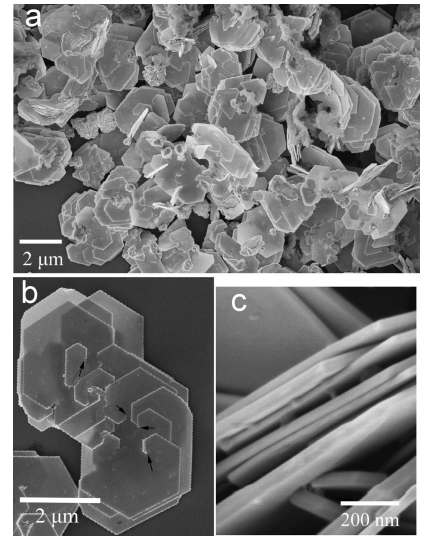

Figure 1. SEM images of the as-synthesized layered assemblies of gold nanoplates at (a) low magnification and (b) high magnification. The steps on the gold nanoplates are labeled by arrows. (c) Lateral section of a single layered assembly.

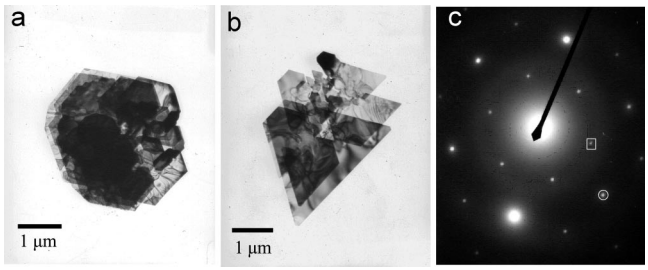

Figure 2. TEM images of the layered assemblies of gold nanoplates with (a) hexagonal and (b) triangular outline, respectively. (c) SAED pattern of a single layer in the assembly; the spots marked with a circle and a square are indexed to {220} and 1/3{422} diffraction spots of fcc gold.

gold (Joint Committee on Powder Diffraction Standards File: 04-0784), which is much stronger than those of the {200} and {220} diffractions. These observations indicate the highly anisotropic nature of the obtained gold layered assemblies and their basal {111} facets preferentially orienting parallel to the supporting surface.

The UV−vis−NIR spectroscopic method was also used to mirror the morphological character of the obtained gold product because gold nanoparticles with different shapes exhibit a SPR band at different frequencies. The corresponding spectrum exhibits two asymmetric absorption bands centering at around 750 and 950 nm (Supporting Information, Figure S4), which could be ascribed to the transverse and longitudinal plasmon resonances respectively arising from the high anisotropy of these layered gold assemblies.

TEM Monitoring of the Formation of Layered Assemblies of Gold Nanoplates. Figure 3 shows TEM images of the samples that were taken from the reaction solution at different intervals. Before aqueous aniline was injected into the flask, the aqueous $HAuCl_4$−HCl solution was light yellow. There was no color change upon mixing the aqueous aniline with the $HAuCl_4$−HCl solution. However, the light-yellow reaction solution became colorless gradually after a reaction time of 3 h. The loss of solution color could be attributed to the reduction of Au^{3+} to Au^{+} by aniline. At this stage, sea-urchin-like aggregates composed of nanobars were observed (Figure 3a) and the corresponding SEAD pattern (Figure 3b) is not consistent with that of metallic gold crystals. It is worth mentioning that Ravishankar et al. previously reported that partial reduction (Au^{3+} to Au^{+}) of $HAuCl_4$ by alkylamine results in a cube-shaped intermediate.[29] We thus presume that these nanobar aggregates could be the complexes of Au^{+} and oligoaniline. When $HAuCl_4$−HCl and aniline solutions were mixed for 6 h, the reaction system turned brownish red and small gold nanoparticles several tens of nanometers in size were formed (Figure 3c). The fcc gold crystal character of these nanoparticles was further confirmed by the corresponding SEAD pattern (Figure 3d). After being mixed for 9 h, the reaction system turned brownish yellow and the gold nanoparticles were evolved into the layered nanoplates with irregular edges. When the mixing time reached 12 h, the reaction solution turned deeply brownish yellow, indicating that the layered assemblies of gold nanoplates continuously grew (Figure 3e). With the time expanding to 15 h, it can be seen that both the layer number and the length edge of the layered assemblies increased (Figure 3f). When $HAuCl_4$−HCl and aniline were mixed for 18 h, the layered assemblies of gold nanoplates with sharp edges can be seen (Figure 3g) and there was no obvious increase in length edge after 18 h of mixing.

Effect of the Amount of Aniline. To investigate the effects of the amount of aniline on the morphology of the gold products, the molar ratio of aniline to gold was varied from 2 to 9 while other reaction conditions reminded constant. Experimental results suggest that the synthesis of layered assemblies of gold nanoplates is insensitive to the amount of aniline. As shown in Figure 4, most of the obtained gold products are also layered assemblies of nanoplates. However, it can be seen that the edge length of the obtained assemblies decreased with the increase in molar ratio of aniline to gold, which may be explained by the number of gold seeds generated at the nucleation step increasing at a higher reductant concentration and thus leading to small sized gold product.

Effect of pH Value of Aqueous $HAuCl_4$. To investigate the effect of initial pH value on the final gold products, the pH value of $HAuCl_4$ solution was adjusted by HCl from pH 0.82 to pH 3.4 by adding aqueous 1 M HCl before reaction.[30] Taking the gold layered assemblies obtained in synthesis at a pH of 1.0 as reference, it is found the layered assemblies of gold nanoplates obtained at a decreased pH value had a longer edge length (Figure 5a), whereas the edge length of the gold product got shorter at an increased pH value (Figure 5b). When the pH value is further increased to pH 1.8, the obtained gold product obtained an extended multilayer structure similar to that of natural nacreous shell,[31] which possesses tens of layers with each layer (gold nanplate) having a submicron edge length (Figure 5c). In particular, the reduction rate of $AuCl_4^-$ got much faster without adding HCl, resulting in rod-like gold nanoparticles with rough surfaces (Figure 5d).

Effect of Reaction Temperature. Investigation indicates that increasing temperature is unfavorable for the formation of layered assemblies of gold nanoplates. For example, when the synthetic procedure was operated at 60 °C, the initial light yellow reaction solution at a pH of 1.0 quickly changed to colorless (Au^{3+} to Au^{+}), and then purple (Au^{+} to Au^{0}), followed by a brownish yellow (growth) within 2 h, indicating a much higher rate of reduction compared with that at room temperature. As measured by SEM (Figure 6a), the final gold products are mainly dispersed gold nanoplates with some spherical nanoparticles as byproduct, and no layered assemblies of gold nanoplates are observed. As temperature was further increased to 80 °C, we achieved a similar result, except that these dispersed gold nanoplates have a smaller edge size than those obtained at 60 °C (Figure 6b). The above experimental results infer that although increasing temperature in a wide range keeps the nucleation and growth in kinetic control, the corresponding reduction rate is still too fast to be favorable for the generation of steps on the gold plates for forming layered assemblies.

Effect of Inorganic Acid. To investigate the effect of the different inorganic acids on the shape of the final gold products, other aqueous 1 M inorganic acids, including HNO_3, H_2SO_4, and $HClO_4$, respectively, were used as an acidity modifier to adjust aqueous $HAuCl_4$ at a pH of 1.0 instead of HCl. In each experiment upon adding aniline, the initial light yellow reaction solution turned from colorless to reddish orange gradually and then gray-blue during a range of 6−8 h, and there was no further change of color, indicating a higher reaction rate than that of the experiment with HCl. Moreover, the gray-blue reaction solution also indicates that the final gold product might possess a shape varied from that obtained with HCl. Figure 7 presents SEM images of the samples synthesized in the presence of HNO_3, H_2SO_4, and $HClO_4$, clearly showing that these gold layered assemblies hold a flower-like shape. Taking account for that the four inorganic acids are all strong and the pH

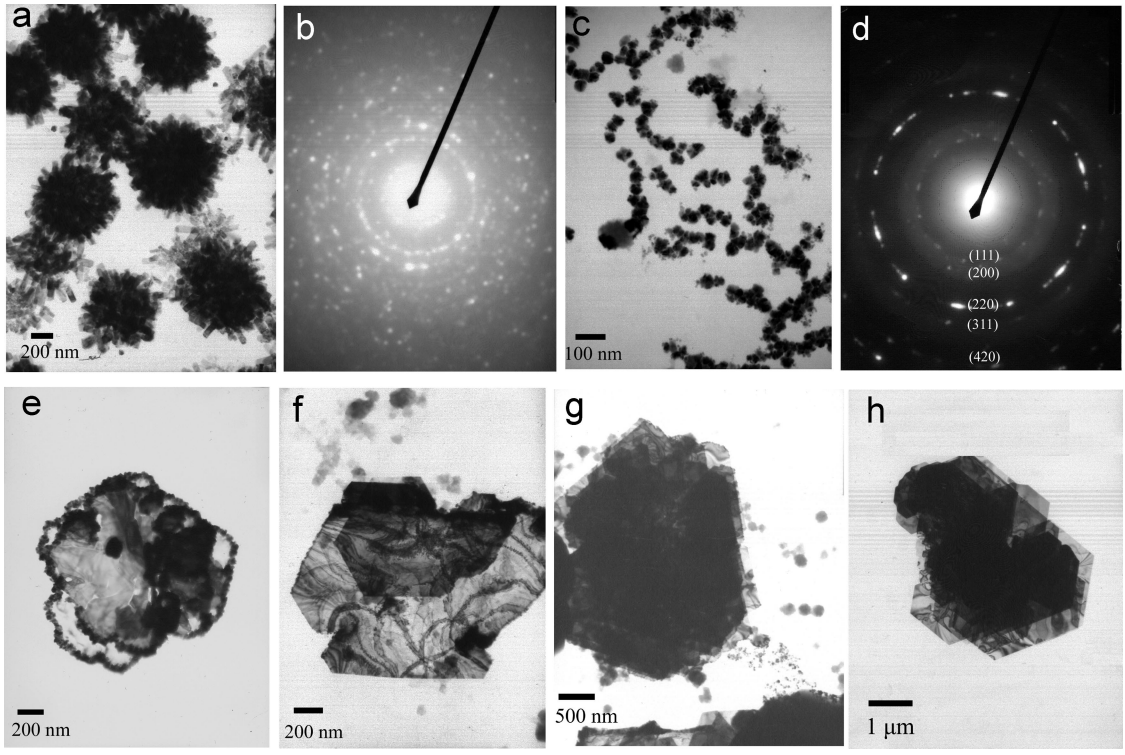

Figure 3. TEM images obtained during different reaction intervals after the mix of $HAuCl_4$−HCl solution with aniline solution for (a) 3, (c) 6, (e) 9, (f) 12, (g) 15, and (h) 18 h. (b) SAED pattern of panel a. (d) SAED pattern of panel c.

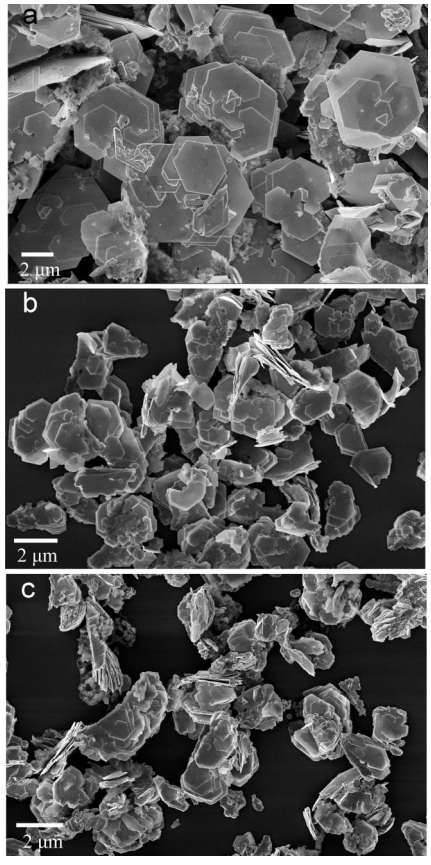

Figure 4. SEM images of the gold product obtained with a (a) 2:1, (b) 6:1, and (c) 9:1 mol ratio of aniline to gold.

(namely H^+ concentration) of each reaction solution is the same, therefore, the Cl^- has a special function relative to NO_3^-, ClO_4^-, and SO_4^{2-}. That is, the presence of Cl^- can greatly slow up the reduction process of $AuCl_4^-$ compared with that of the other three anions. The initial explanation lies on the oxidizing action of the O_2/Cl^- pair:[23] The Cl^- can couple with the O_2 dissolved in solution to form the O_2/Cl^- pair. When using HCl as an acidity modifier, the presence of a large amount of H^+ as well as Cl^- can highly enhance the oxidation ability of the O_2/Cl^- pair, which is supported by the following standard electrical potential eqs 1 and 2:[32]

$$O_2+4H^++4e^-=2H_2O \quad E^0=1.229\ \text{V} \tag{1}$$

$$O_2+2H_2O+4e^-=4OH^- \quad E^0=1.401\ \text{V} \tag{2}$$

The extensive oxidizing power of the O_2/Cl^- pair could oxidize gold atoms back to gold salts, competing with the reduction process of $AuCl_4^-$, and thus reducing the whole formation rate of gold atoms (standard electrical potential eqs 3 and 4).[32] This might lead to the nucleation and growth of gold crystal in a quite slow rate, resulting in the gold layered assemblies with regular edges.

$$AuCl_4^-+2e^-=AuCl_2^-+2Cl^- \quad E^0=0.926\ \text{V} \tag{3}$$

$$AuCl_2^-+e^-=Au+2Cl^- \quad E^0=1.15\ \text{V} \tag{4}$$

However, it should not be neglected that NO_3^- and ClO_4^- also have mild or even strong oxidation ability in acid solution that could affect the reduction rate of $AuCl_4^-$, which is supported by the standard potential eqs 5−7:[32]

$$ClO_4^-+2H^++2e^-=ClO_3^-+H_2O \quad E^0=1.201\ \text{V} \tag{5}$$

$$NO_3^-+3H^++2e^-=NHO_2+H_2O \quad E^0=0.94\ \text{V} \tag{6}$$

$$SO_4^{2-}+4H^++2e^-=SO_2(aq)+H_2O \quad E^0=0.158\ \text{V} \tag{7}$$

It can be seen that ClO_4^- has a similar oxidizing power as that of the O_2/Cl^- pair by checking their standard potential values. If the O_2/Cl^- pair is the main point for highly slowing

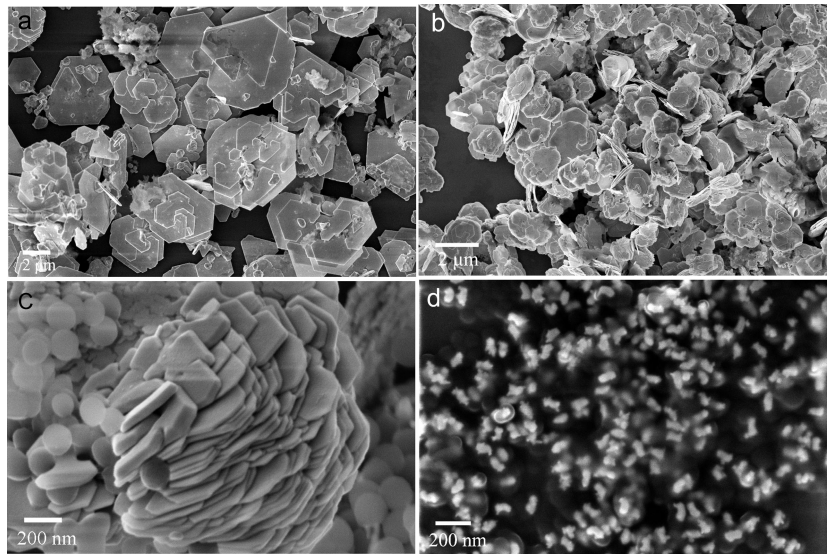

Figure 5. SEM images of gold products obtained at an initial pH of (a) 0.82, (b) 1.3, (c) 1.8, and (d) 3.4.

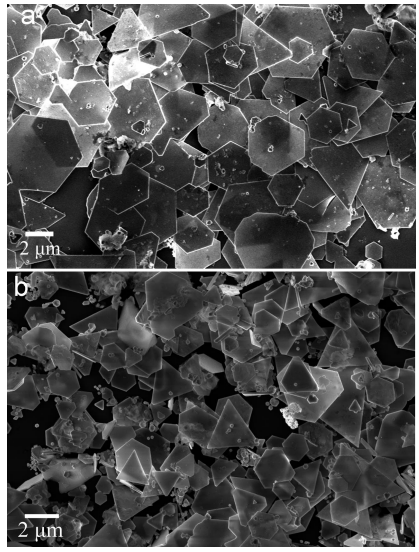

Figure 6. SEM images of dispersed gold nanoplates obtained at a temperature of (a) 60 and (b) 80 °C.

up the reduction rate of gold precursor when using HCl, ClO_4^- should have a similar effect on the reduction rate of $AuCl_4^-$ in the synthesis with $HClO_4$, which is obviously not consistent with the above experimental facts. On the other hand, we also notice that the initial gold precursor $AuCl_4^-$ is a complex ion in which Cl^- acts as a ligand agent. As shown in eqs 3 and 4, each step of the reduction of gold precursor is companied by the release of Cl^-. According to chemical equilibrium principle, increasing the concentration of Cl^- can inhibit the reduction process of $AuCl_4^-$ and thus slow up the reduction rate. In our case operated at a pH of 1.0, the mole ratio of Cl^- to gold ions is about 138:1 before reaction when using HCl. Thus it is believed that the overwhelming excess of Cl^- plays a key role in a quite slow reduction process of gold ions, whereas the O_2/Cl^- pair only has a limited effect on the reduction rate, and the same with ClO_4^- and NO_3^-.

Formation Mechanism. On the basis of the above experimental results, a possible formation mechanism for layered assemblies of gold nanoplates via our approach can be proposed. In the room temperature synthesis of gold nanostructures at a pH of 1.0 adjusted by HCl, the reduction rate of gold ions turns much slow due to the following factors: (1) the presence of a large amount Cl^-; (2) oxidative etching by the O_2/Cl^- pair; (3) the protonation of aniline; and (4) the mild reaction temperature. Hence the nucleation and growth of gold crystals is subject to kinetic control. Meanwhile, the in situ produced polyaniline preferentially adsorbs on the {111} facets of the gold seeds through their nirtogenous groups and prevents the growth of these facets, inducing other facets such as {100} or {110} facets to grow more quickly. Hence, gold nanoplates bounded mainly by {111} facets are gradually formed. On the other hand, these polyaniline produced in the present synthesis possess a rigidly straight chain molecular structure. Such molecular configuration induces each polyaniline molecule to only adsorb the crystal facet within one-dimensional space and thus has an insufficient capping effect on preventing the growth of {111} facets compared with the flexible ones. Hence during the growth of a nanoplate, some steps (namely stacking faults) would generate along the ⟨111⟩ direction on the basal surface of the nanoplate and serve as active growth sites to form new nanoplates, resulting in the formation of the layered assemblies of gold nanoplates. Moreover, if the rigidly straight polyaniline molecules indeed induce incomplete coverage on the {111} facets of gold nanoplates, introducing an extra capping agent with flexible molecular structure to fill up the uncapped sites would be capable of preventing the occurrence of these steps. In the following experiments, we chose PVP, which preferentially adsorbs on the {111} facets of the gold nanocrystals,[33] as an assistant capping agent[34] to introduce into the reaction system to investigate the morphology change of final gold product. The experimental results clearly reveal that most of the obtained gold products are dispersed gold nanoplates but not their layered assemblies (Figure 8), consistent with the above-proposed mechanism. Also, this reveals that the formation of the gold layered assemblies by Yuan's approach also follows this mechanism in nature: (1) The doped SPANI can be regarded as the protonation of SPANI to induce a quite slow reduction rate, which is also supported by the fact that using dedoped SPANI nanotubes instead of doped ones only gave dispersed gold nanoparticles and nanoplates.[18] (2) During the reaction process, the SPANI segments degraded from doped SPANI nanotubes worked as a capping agent to preferentially adsorb on the {111} facets of the gold seeds. (3) The SPANI segments also possess rigidly straight molecular structure and thus

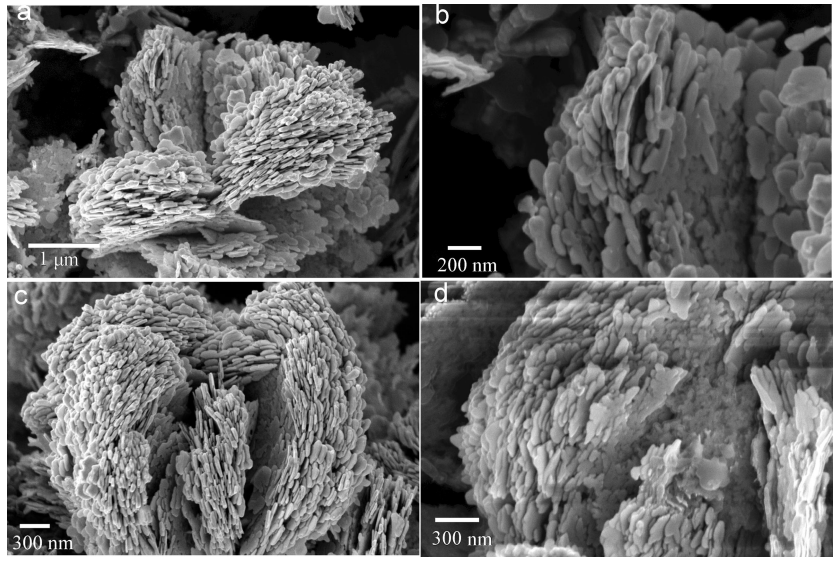

Figure 7. SEM images of the as-synthesized gold products in the presence of (a) HNO_3, (c) H_2SO_4, and (d) $HClO_4$. (b) High magnification of panel a.

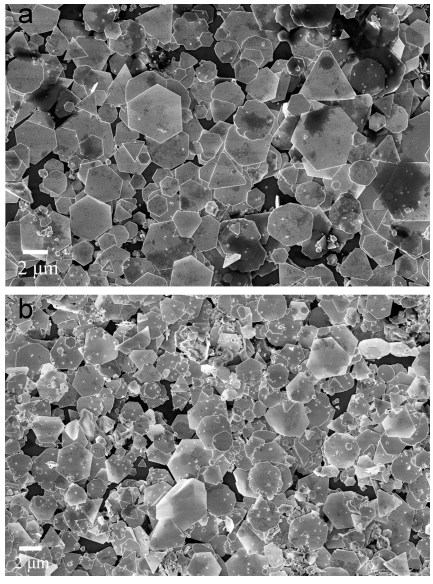

Figure 8. SEM images of dispersed gold nanoplates obtained in the presence of PVP with a (a) 2:1 and (b) 5:1 mol ratio of the repeating unit to gold.

incompletely absorb on the {111} facets, resulting in the formation of the gold layered assemblies.

Conclusion

In summary, we have developed a simple room temperature approach to directly synthesize the layered assemblies of single crystal gold nanoplates with regular edges through a slow-growth process based on the reduction of aqueous $HAuCl_4$−HCl by aniline, without additional capping agent or surfactant. Remarkably, the as-synthesized gold layered assemblies are composed of inseparable nanoplates connected to each other by steps between layers, which make them stable in solution even after extensive ultrasonic treatment. During this slow-growth process, the in situ produced polyaniline with rigidly straight chain molecular structure plays a key role in achieving these layered assemblies by selectively but incompletely adsorbing on {111} facets of gold nanocrystals, which facilitates the generation of steps on {111} facets, resulting in the final gold product with layered structure. Investigation reveals that the shape or size of the final gold nanostructures can be influenced by the amount of aniline, the initial pH value, the reaction temperature, and the inorganic acid. The synthesis and product are important because they not only provide a convenient route to ordered assemblies of anisotropic gold nanoparticles for various applications, but also add a clue to further understanding the mechanism for crystal growth.

Acknowledgment. This work was supported by the National Natural Science Foundation of China (90406023, 60571031, and 60501009) and the National Important Basic Research Program of China (2006CB933206 and 2006CB705606).

Supporting Information Available: EDX spectrum, FT-IR spectrum, UV−vis−NIR spectrum, and XRD pattern of as-synthesized layered assemblies of gold nanoplates. This material is available free of charge via the Internet at http://pubs.acs.org.

References and Notes

(1) (a) Schmid, G. *Chem. Rev.* **1992**, *92*, 1709. (b) Bönnemann, H.; Richards, R. M. *Eur. J. Inorg. Chem.* **2001**, 2455. (c) Roucoux, A.; Schulz, J.; Patin, H. *Chem. Rev.* **2002**, *102*, 3757. (d) Daniel, M. C.; Astruc, D. *Chem. Rev.* **2004**, *104*, 293.

(2) (a) EL-Sayed, M. A. *Acc. Chem. Res.* **2001**, *34*, 257. (b) Kelly, K. L.; Coronado, E.; Zhao, L.; Schatz, G. C. *J. Phys. Chem. B* **2003**, *107*, 668. (c) Eustis, S.; El-Sayed, M. A. *Chem. Soc. Rev.* **2006**, *35*, 209.

(3) Liz-Marzán, L. M. *Langmuir* **2006**, *22*, 32.

(4) Tian, N.; Zhou, Z.; Sun, S.; Ding, Y.; Wang, Z. *Science* **2007**, *316*, 732.

(5) (a) Ahmadi, T. S.; Wang, Z. L.; Green, T. C.; Heglein, A.; El-Sayed, M. A. *Science* **1996**, *272*, 1924. (b) Kim, F.; Connor, S.; Song, H.; Kuykendall, T.; Yang, P. *Angew. Chem., Int. Ed.* **2004**, *43*, 3673. (c) Sun, Y.; Xia, Y. *Science* **2002**, *298*, 2176. (d) Chen, Y.; Gu, X.; Nie, C.; Jiang, Z.; Xie, Z.; Lin, C. *Chem. Commun.* **2005**, 4181. (e) Zhou, M.; Chen, S.; Zhao, S. *J. Phys. Chem. B* **2006**, *110*, 4510. (f) Seo, D.; Park, J. C.; Song, H. *J. Am. Chem. Soc.* **2006**, *128*, 14863.

(6) (a) Lisiecki, I.; Filankembo, A. *Phys. Rev. B: Condens. Matter* **2000**, *61*, 4968. (b) Jana, N. R.; Gearheart, L.; Murphy, C. J. *J. Phys. Chem. B* **2001**, *105*, 4065. (c) Sun, Y.; Gates, B.; Mayers, B.; Xia, Y. *Nano Lett.* **2002**, *2*, 165. (d) Fu, X.; Wang, Y.; Wu, N.; Gui, L.; Tang, Y. *J. Mater. Chem.* **2003**, *13*, 1192. (e) Vasilev, K.; Zhu, T.; Wilms, M.; Gillies, G.; Lieberwirth, I.; Mittler, S.; Knoll, W.; Kreiter, M. *Langmuir* **2005**, *21*, 12399. (f) Zhang, J.; Du, J.; Han, B.; Liu, Z.; Jiang, T.; Zhang, Z. *Angew. Chem., Int. Ed.* **2006**, *45*, 1116. (g) Chen, J.; Wiley, B. J.; Xia, Y. *Langmuir* **2007**, *23*, 4120.

(7) (a) Jin, R. C.; Cao, Y.; Mirkin, C. A.; Kelly, K. L.; Schatz, G. C.; Zheng, J. G. *Science* **2001**, *294*, 1901. (b) Chen, S.; Fan, Z.; Carroll, D. L.

J. Phys. Chem. B **2002**, *106*, 10777. (c) Shankar, S. S.; Rai, A.; Ankamwar, B.; Singh, A.; Ahmad, A.; Sastry, M. *Nat. Mater.* **2004**, *3*, 482. (d) Shao, Y.; Jin, Y.; Dong, S. *Chem. Commun.* **2004**, 1104. (e) Li, Z.; Liu, Z.; Zhang, J.; Han, B.; Du, J.; Gao, Y.; Jiang, T. *J. Phys. Chem. B* **2005**, *109*, 14445. (f) Millstone, J. E.; Park, S.; Shuford, K. L.; Qin, L.; Schatz, G. C.; Mirkin, C. A. *J. Am. Chem. Soc.* **2005**, *127*, 5312. (g) Li, C.; Cai, W.; Cao, B.; Sun, F.; Li, Y.; Kan, C.; Zhang, L. *Adv. Funct. Mater.* **2006**, *16*, 83. (h) Huang, W.; Chen, C.; Huang, M. H. *J. Phys. Chem. C* **2007**, *111*, 2533.

(8) (a) Hao, E.; Bailey, R. C.; Schatz, G. C.; Hupp, J. T.; Li, S. *Nano. Lett.* **2004**, *4*, 327. (b) Teng, X.; Yang, H. *Nano Lett.* **2005**, *5*, 885. (c) Bakr, O. M.; Wunsch, B. H.; Stellacci, F. *Chem. Mater.* **2006**, *18*, 3297. (d) Lou, X.; Yuan, C.; Archer, L. A. *Chem. Mater.* **2006**, *18*, 3921. (e) Yuan, H.; Ma, W.; Chen, C.; Zhao, J.; Liu, J.; Zhu, H.; Gao, X. *Chem. Mater.* **2007**, *19*, 1592.

(9) Murray, C. B.; Kagan, C. R. *Annu. Rev. Mater. Sci.* **2000**, *30*, 545.

(10) See, for example: (a) Rao, C. N. R.; Kulkarni, G. U.; Thomasa, P. J.; Edwards, P. P. *Chem. Soc. Rev.* **2000**, *29*, 27. (b) Pileni, M. P. *J. Phys. Chem. B* **2001**, *105*, 3358. (c) Schmid, G.; Simon, U. *Chem. Commun.* **2005**, 697. (d) Tang, Z.; Kotov, N. A. *Adv. Mater.* **2005**, *17*, 951.

(11) (a) Murphy, C. J.; Sau, T. K.; Gole, A. M.; Orendorff, C. J.; Gao, J.; Gou, L.; Hunyadi, S. E.; Li, T. *J. Phys. Chem. B* **2005**, *109*, 13857. (b) Joseph, S. T. S.; Ipe, B. I.; Pramod, P.; Thomas, K. G. *J. Phys. Chem. B* **2006**, *110*, 150. (c) Rajeev Kumar, V. R.; Samal, A. K.; Sreeprasad, T. S.; Pradeep, T. *Langmuir* **2007**, *23*, 8667. (d) Sreeprasad, T. S.; Samal, A. K.; Pradeep, T. *Langmuir* **2008**, *24*, 4589.

(12) Ankamwar, B.; Chaudhary, M.; Sastry, M. *Synth. React. Inorg. Met.-Org. Chem.* **2005**, *35*, 19.

(13) Shankar, S. S.; Rai, A.; Ahmad, A.; Sastry, M. *Chem. Mater.* **2005**, *17*, 566.

(14) Wang, T.; Hu, X.; Dong, S. *J. Phys. Chem. B* **2006**, *110*, 16930.

(15) Dahanayaka, D. H.; Wang, J. X.; Hossain, S.; Bumm, L. A. *J. Am. Chem. Soc.* **2006**, *128*, 6052.

(16) Yun, Y. J.; Park, G. *Appl. Phys. Lett.* **2005**, *87*, 233110.

(17) Malikova, N.; Pastoriza-Santos, I.; Schierhorn, M.; Kotov, N. A.; Liz-Marzán, L. M. *Langmuir* **2002**, *18*, 3694.

(18) Yuan, J.; Wang, Z.; Zhang, Q.; Han, D.; Zhang, Y.; Shen, Y.; Niu, L. *Nanotechnology* **2006**, *17*, 2641.

(19) MacDiarmid, A. G. *Synth. Met.* **2002**, *125*, 11.

(20) (a) Nakao, H.; Shiigi, H.; Yamamoto, Y.; Tokonami, S.; Nagaoka, T.; Sugiyama, S.; Ohtani, T. *Nano Lett.* **2003**, *3*, 1391. (b) Kinyanjui, J. M.; Hatchett, D. W. *Chem. Mater.* **2004**, *16*, 3390. (c) Mallick, K.; Witcomb, M. J.; Dinsmore, A.; Scurrell, M. S. *Macromol. Rapid Commun.* **2005**, *26*, 232. (d) Subramaniam, C.; Tom, R. T.; Pradeep, T. *J. Nanopart. Res.* **2005**, *7*, 209. (e) Zheng, G.; Shao, Y.; Xu, B. *Acta Chim. Sinica* **2006**, *64*, 733.

(21) Guo, Z.; Zhang, Y.; Huang, L.; Wang, M.; Wang, J.; Sun, J.; Xu, L.; Gu, N. *J. Colloid Interface Sci.* **2007**, *309*, 518.

(22) Liu, G.; Freund, M. S. *Macromolecules* **1997**, *30*, 5660.

(23) Gospodinova, N.; Terlemezyan, L. *Prog. Polym. Sci.* **1998**, *23*, 1443.

(24) (a) Petroski, J. M.; Wang, Z.; Green, T. C.; El-Sayed, M. A. *J. Phys. Chem. B* **1998**, *102*, 3316. (b) Peng, X.; Manna, L.; Yang, E.; Wickham, J.; Scher, E.; Kadavanich, A.; Alivisatos, A. P. *Nature* **2000**, *404*, 59. (c) Jun, Y.; Jung, Y.; Cheon, J. *J. Am. Chem. Soc.* **2002**, *124*, 615. (d) Xiong, Y.; McLellan, J. M.; Chen, J.; Yin, Y.; Li, Z.; Xia, Y. *J. Am. Chem. Soc.* **2005**, *127*, 17118.

(25) Wang, Z. L. *J. Phys. Chem. B* **2000**, *104*, 1153.

(26) Zhang, J.; Ma, F.; Xu, K. *Appl. Surf. Sci.* **2004**, *229*, 34.

(27) Tao, A. R.; Habas, S.; Yang, P. *Small* **2008**, *4*, 310, and references cited therein.

(28) Tan, Y.; Li, Y.; Zhu, D. *J. Colloid Interface Sci.* **2003**, *258*, 244.

(29) Halder, A.; Ravishankar, N. *J. Phys. Chem. B* **2006**, *110*, 6595.

(30) Because of the intrinsic acidity of $HAuCl_4$, the pH value of 0.72 mM aqueous $HAuCl_4$ is 3.4.

(31) Mayer, G. *Science* **2005**, *310*, 1144.

(32) Dean, J. A. *Lange's Handbook of Chemistry*, 15th ed.; McGraw-Hill: New York, 1999.

(33) (a) Tsuji, M.; Hashimoto, M.; Nishizawa, Y.; Kubokawa, M.; Tsuji, T. *Chem. Eur. J.* **2005**, *11*, 440. (b) Kan, C.; Zhu, X.; Wang, G. *J. Phys. Chem. B* **2006**, *110*, 4651.

(34) Recently some studies have suggested that PVP can also react with $HAuCl_4$ to form gold nanoparticles (see, for example: (a) Xiong, Y.; Washio, I.; Chen, J.; Cai, H.; Li, Z.; Xia, Y. *Langmuir* **2006**, *22*, 8563. (b) Hoppe, C. E.; Lazzari, M.; Pardiñas-Blanco, I.; López-Quintela, M. A. *Langmuir* **2006**, *22*, 7027.). However, our control experiments indicate that adding PVP to $HAuCl_4$−HCl aqueous solution at pH 1.0 without the presence of aniline cannot induce the reduction of $AuCl_4^-$ during the whole reaction time at room temperature.

JP8028962